TUTORIAL-REVIEW

Experimental Consideration of Two-Dimensional Fourier Transform Spectroscopy

Liang Zhou, Lie Tian, Wen-kai Zhang*

Department of Physics and Applied Optics Beijing Area Major Laboratory, Center for Advanced Quantum Studies, Beijing Normal University, Beijing 100875, China

(Dated: Received on July 19, 2020; Accepted on August 19, 2020)

Two-dimensional Fourier transform (2D FT) spectroscopy is an important technology that developed in recent decades and has many advantages over other ultrafast spectroscopy methods. Although 2D FT spectroscopy provides great opportunities for studying various complex systems, the experimental implementation and theoretical description of 2D FT spectroscopy measurement still face many challenges, which limits their wide application. Recently, the 2D FT spectroscopy reaches maturity due to many new developments which greatly reduces the technical barrier in the experimental implementation of the 2D FT spectrometer. There have been several different approaches developed for the optical design of the 2D FT spectrometer, each with its own advantages and limitations. Thus, a procedure to help an experimentalist to build a 2D FT spectroscopy experimental apparatus is needed. This tutorial review is intending to provide an accessible introduction for a beginner to build a 2D FT spectrometer.

Key words: Two-dimensional Fourier transform spectroscopy, Two-dimensional infrared spectroscopy, Two-dimensional electronic spectroscopy

I. INTRODUCTION

Ultrafast spectroscopy techniques have achieved great success in the past few decades. With the development of pump-probe spectroscopy, many different ultrafast spectroscopy methods have been used to study various population dynamics and coherent dynamics [1−4]. However, there is a trade-off between time and frequency resolution in most ultrafast spectrometry. In order to obtain a higher time resolution, a shorter pump pulse is required, which corresponds to a broader bandwidth due to the restriction of the time-bandwidth product. Thus, it is hard to specify the excitation frequency with higher certainty. It produces a significant difficulty in following the specific ultrafast dynamics process in a pump-probe measurement. This trade-off is circumvented by coherent multi-dimensional Fourier transform (MD FT) spectroscopy. The first MD FT spectroscopy experimental demonstration is the two-dimensional Fourier transform (2D FT) spectroscopy. There are effectively three light-matter interactions in a 2D FT spectroscopy measurement. The 2D FT spectroscopy can access some details which are not generally accessible in one-dimensional spectra. Nowadays, the 2D FT spectroscopy has become a mature technology with broad application. A variety of 2D FT spectroscopy methods have been developed and applied in chemistry, physics, biophysics, and material science [5−28]. Many excellent reviews and book chapters have been devoted to introducing the principles and recent applications of 2D FT spectroscopy [29−47]. However, a procedure for a beginner who wants to build a 2D FT spectrometer is still lacking. So, this tutorial review is intending to fill this gap. In this review, we first give an overview of the 2D FT spectroscopy and discuss the typical challenges of implementing the 2D FT spectrometer from the perspective of experimentalists. Then we outline five typical optical designs of the 2D FT spectrometer, then compare the benefits and drawbacks of these setups. At last, the future and perspective of 2D FT spectroscopy development are given. We hope this review can provide an accessible introduction for a beginner who wants to build a 2D FT spectrometer.

II. 2D FT SPECTROSCOPY OVERVIEW

In a pump-probe experiment, the change induced by the pump pulse is detected by the probe pulse after a waiting time T (FIG. 1(a)). The signal we acquire is a function of the waiting time T, and the time resolution depending on the pulse duration of the pump pulse. However, a shorter pump pulse has broader bandwidth due to the restriction of the time-bandwidth product. So, it is impossible to have higher time resolution and higher certainty of the excitation frequency simultane-

*Author to whom correspondence should be addressed. E-mail: wkzhang@bnu.edu.cn

ously, which is also inevitable, it needs to be balanced within the pump-probe experiment. The core of the problem is how to excite a specific system with high-frequency precision while keeping a high time resolution at the same time. Inspired by multi-dimensional nuclear magnetic resonance (NMR), researchers started to develop the 2D spectrometer. It is worth noting that the 2D FT spectroscopy is a different technique from 2D correlation spectroscopy. 2D correlation spectroscopy is a mathematical technique that is used to study changes in measured signals. In which, a series of perturbation-induced dynamic one-dimensional spectra are collected and transformed into a set of 2D correlation spectra by simple cross-correlation analysis [48]. However, 2D FT spectroscopy directly measures the time evolution of the three-order nonlinear response of the system. Hochstrasser and coworkers adopted the burning-hole method to record the 2D spectroscopy by scanning the full energy mode with a narrowband pump pulse [49]. The major disadvantage of this method is that the long pulse duration of the narrowband pump pulse generally leads to a poor time resolution. Recently, Zheng and coworkers demonstrated that the three-dimensional molecular conformations and their population distributions of a molecule could be successfully mapped by analyzing the relative orientations of the transition dipole moments of normal modes which cover the molecular space of all chemical bonds using frequency-domain 2D FT spectroscopy in a broad frequency range from 1000 cm^{-1} to 3200 cm^{-1} [50].

One can also collect 2D spectroscopy in the time domains by scanning the time delay between a pair of broadband pulses. FIG. 1(b) shows a typical pulse sequence in the 2D FT spectroscopy experiment. The pulse 1 and 2 are two coherent pump pulses; the pulse 3 is a probe pulse to inquire about the system. The radiated three-order nonlinear signal field $E_{\rm sig}$ could be written as

$$\begin{aligned} & E_{\rm sig}(k_{\rm sig},t) \propto iP^{(3)}(k_{\rm sig},t) \\ = & \int_0^\infty {\rm d}t_3 \int_0^\infty {\rm d}t_2 \int_0^\infty {\rm d}t_1 R^{(3)}(t_3,t_2,t_1) E_3(k_3,t-t_3) \\ & E_2(k_2,t-t_3-t_2) E_1(k_1,t-t_3-t_2-t_1) \end{aligned} \quad (1)$$

The response function $R^{(3)}(t_3,t_2,t_1)$ could be written as a nested commutator of the transition dipole operator $\mu(t)$ as follows:

$$\begin{aligned} & R^{(3)}(t_3,t_2,t_1) \\ = & \left(\frac{i}{\hbar}\right)^3 \langle [[[\mu(t_3+t_2+t_1),\mu(t_2+t_1)],\mu(t_1)],\mu(0)]\rangle \end{aligned} \quad (2)$$

The pulse 4 is a local oscillator for heterodyne detecting of the signal in non-collinear geometry. In some fully or partially colinear geometries, the role of pulse 4 usually is replaced by the probe pulse. The time delay between the pump pulses 1 and 2 is coherence time τ, and the time delay between the pulse 3 and 4 is local oscillator time t. The time delay between pulse 2 and pulse 3 is the waiting time T, which is similar to the pump-probe experiment. The 2D frequency-frequency contour plots for a given waiting time T is the Fourier transform of the 2D signal for the τ and t. In practice, the local oscillator time t axis is Fourier transformed during data collection by the monochromator, and the coherence time τ axis is numerically Fourier transformed after data acquisition is finished. So, the excitation frequency is correlated to the coherence time by Fourier transform. The coherence time τ should be scanned to get all excitation frequencies, as shown in FIG. 1(c). And the time resolution is still decided by the pulse duration of the pump pulse. Thus, we could get a precise excitation frequency while keeping a short pulse duration at the same time, which means we could have both high time and frequency resolution simultaneously.

FIG. 1(d) shows a typical fully non-collinear phase-matching geometry, the box-CARS geometry, which has been used in many 2D FT spectroscopy measurements [30]. In the box-CARS geometry, the wave vectors of three excitation pulses and the emitted signal form a square. Therefore, the signal is almost background free since it is completely separated from the excitation pulses and most other nonlinear emissions. A spectral interferogram including the phase and amplitude information of the complex nonlinear signals is recorded using heterodyne detection by directing a local oscillator beam to this fourth corner. In box-CARS geometry, two typical phase-matched signals are recorded: the rephasing signal in the $k_2-k_1+k_3$ direction and the non-rephasing signal in the $k_1-k_2+k_3$ direction. A pure absorption 2D FT spectroscopy could be obtained by summing the rephasing and non-rephasing signal together. The pure absorptive spectra have the highest frequency resolution, and there is no phase twist that can distort spectra. The analysis of the line shape from the pure absorption 2D FT spectrum could get some critical information such as inhomogeneous and homogenous linewidthes which has an essential connection with molecular microscopic dynamics [51−54].

A significant consideration when designing a 2D FT spectrometer is phase drift. In order to avoid phase drift, it is essential to maintain phase stability between pulses. Phase stability refers to the phase variation of one pulse relative to another within a given time delay. Therefore, the relative timescale of phase stability is determined by the oscillation period of the light field. As a consequence, it is relatively straightforward to maintain phase stability for infrared (IR) and even longer wavelengths, Still, it is more challenging and has become a more demanding instrumentation consideration with regards to visible and even higher frequency pulses. In a typical 2D FT spectroscopy, it is essential to maintain phase stability for the time delays τ and t since the system is in a coherence state, but it is less important for the waiting time delays T since the system is in a population state. Generally, the coherence time

DOI:10.1063/1674-0068/cjcp2007125

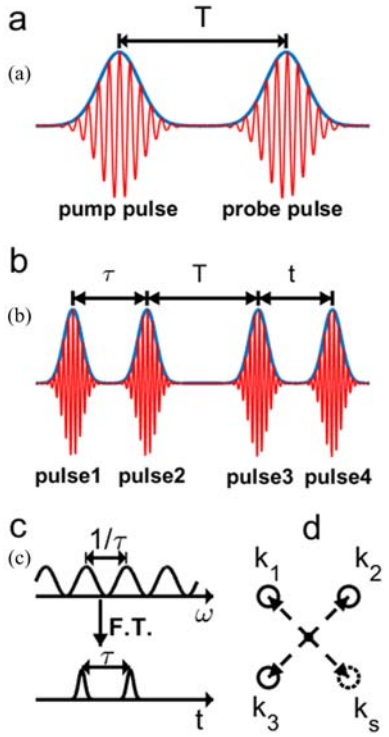

FIG. 1 The pulse sequence of (a) the pump-probe experiment and (b) the 2D FT experiment. (c) The principle of Fourier transforms in the 2D FT spectroscopy. (d) The box-CARS phase matching geometries. The arrows show the directions of the pulses relative to the focus at the sample, which is marked with a hatched circle.

τ is scanned in the time domain, then converted to the excitation frequency by Fourier transform. In order to convert the time delay to an accurate Fourier transform frequency, an interferometric precision of $\sim\lambda/100$ is required, which corresponds to a timing error of $\sim$0.017 fs at 500 nm and a timing error of $\sim$0.17 fs at 5000 nm [34]. The fluctuations of the optical pathlength and mechanical instability are the critical elements that influence phase stability in the experiment. All these elements need to be controlled or compensated to achieve high phase stability. Therefore, many different methods have been successfully developed and applied, which can be roughly divided into two categories: active and passive phase stabilization methods. In this section, we will briefly discuss these two methods and their advantages and limitations.

In most of the 2D FT spectroscopy setups, the most straightforward approach to control the delay between pulses is to have each pulse travel through a separate optical path, in which a linear translation stage can control each delay. The phase stability is naturally reduced in this method since each beam is incident on the different optomechanical components. It can be overcome with active measurement and compensation for the pathlength drift of different beams. A typical active phase stabilization method that usually is used by experimentalists is the reference beam method [30]. Specifically, a continuous-wave (CW) reference beam is used to co-propagate through the optical layout with the excitation beams and the phase of the reference beams is measured just before the sample. The phase drift is compensated by feedback loops to make small changes to the optical path lengths of different beams. The active phase stabilization method can maintain high phase stability as long time as needed and has been used in many 2D FT spectrometers and proved to work well [55−58]. However, the construction of active phase stabilization instruments is nontrivial since it usually requires an electronics device with complicated optical design. So, passive phase stabilization approaches have been widely pursued since it is relatively easy. The pathlengths of different beams can be locked by all beams hitting on common optics, so the relative phase is stabilized. Several passive phase stabilization methods have been developed by making the beam incident on identical optics [59, 60].

Another challenge is that the 2D signal often needs to be isolated from a background field, scattering, or other noises. Three techniques have been developed to solve this problem: amplitude modulation, phase modulation or phase-cycling, and phase matching. For example, Davis and coworkers isolated quantum coherence successfully by amplitude modulation for each pulse [61]. Zanni and coworkers eliminated the scattering using the phase-cycling method since a pure phase inversion is possible when the pump pulse pair is generated by a pulse shaper [62]. Hamm and coworkers demonstrated that the quasi-phase-cycling could be used to eliminate any scattering contamination [63, 64]. Recently, Massari and coworkers developed a fully reflective 2D IR setup, which removed the scatter contribution using fibrillation of multiple pulses in the phase-matched direction [65]. Scattering and other noises can also be eliminated by synchronously chopping one beam like we generally do in regular 2D IR experiments. Augulis and Zigmantas demonstrated that the artifacts or 'ghost' signals could be removed by using two different lock-in choppers to modulate each pump beam [66]. Zhang and coworkers put the lock-in chopper in each pump beam to eliminate the other undesired nonlinear signals in partial colinear geometry [58]. Some or all of these methods are often used in combination, depending on the experimental requirement.

III. TYPICAL EXPERIMENTAL DESIGN OF 2D FT SPECTROSCOPY

In this section, we will introduce five typical experimental designs of the 2D FT spectrometer, including box-CARS geometry, pump-probe geometry with Mach-Zehnder interferometer, pulse shaper, translating-Wedge-based Identical pulse eNcoding system (TWINS), and gradient-assist photo echo (GRAPE). Each optical design has its unique advan-

DOI:10.1063/1674-0068/cjcp2007125

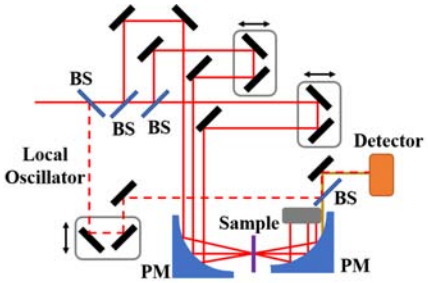

FIG. 2 The optical design of box-CARS geometry. BS: beam splitter, PM: parabolic mirror.

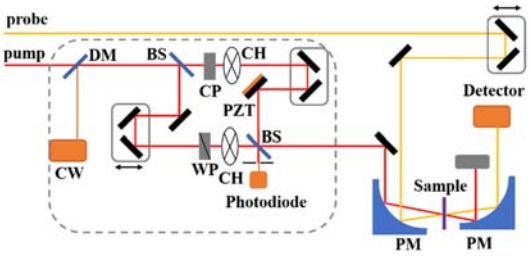

FIG. 3 The optical design of the pump-probe geometry with Mach-Zehnder interferometer. DM: dichroic mirror, BS: beam splitter, CP: compensate plate, WP: wedge plate pair, PZT: piezoelectric transducer, CH: optical chopper, CW: continue-wave, PM: parabolic mirror.

tages and drawbacks. It is essential for experimentalists to choose a proper optical design by comparing their features and technical difficulties.

A. box-CARS geometry

FIG. 2 shows the optical design of the box-CARS geometry. As a fully non-linear geometry, the box-CARS geometry could acquire the 2D FT spectroscopy signal with a free background. Thus, it has a higher SNR than most other optical designs. Each pulse could be controlled independently in box-CARS geometry, so this design provides the maximum freedom to modulate each pulse independently. Although the box-CARS geometry has many unique advantages, there are also some drawbacks and limitations. First, the three-dimensional optical design of the box-CARS geometry creates a huge technical barrier that is hard to overcome for many experimentalists. Second, in order to obtain a pure absorption 2D FT spectrum, the phase relationship between the rephrasing signal and non-rephasing signal needs to be determined. One way of precise phasing is to apply the projection-slice theorem, which can obtain the unknown phase shift using spectrally resolved pump-probe signal [67]. Third, the wedge-based delay line has been used to replace the mechanical delay stage in 2D electronic spectroscopy (2D ES). However, the spectral distortion that arises by the wedge-base delay line is serious and needs to be corrected sometimes. Weng and coworkers demonstrated that spectral distortions could be corrected by an accurately predetermined calibration factor [68].

Although the box-CARS geometry is complicated, the benefits of freedom and high SNR make it the best choice for experienced experimentalists. For example, the ability to control the polarization of each pulse makes the box-CARS geometry the best choice for polarization measurements.

B. Pump-probe geometry with Mach-Zehnder interferometer

Compared to box-CARS geometry, the pump-probe geometry with Mach-Zehnder interferometer (from now on referred to as Mach-Zehnder interferometer geometry, FIG. 3) is a perfect method to balance the technical barrier and freedom [69]. The Mach-Zehnder interferometer geometry has many advantages. First, the collinear propagation design of double excitation pulses reduces the technical barrier of 2D FT spectroscopy significantly. Second, the Mach-Zehnder interferometer geometry still provides great freedom for us to control each beam separately. Third, the Mach-Zehnder interferometer geometry can acquire the pure absorption signal directly. Even the Mach-Zehnder interferometer geometry has many unique advantages; there are also some drawbacks and limitations. The SNR of the Mach-Zehnder interferometer geometry is lower than the box-CARS geometry because of the influence of the background. The 2D FT signal of Mach-Zehnder interferometer geometry usually includes the transient absorption signals produced by pump 1 and pump 2 separately interacting with the probe, which will degrade the data quality. So, these transient absorption signals need to be subtracted using a chopper.

Although the data quality is poor compared to the box-CARS geometry, the Mach-Zehnder interferometer geometry is an excellent optical design and suitable for most experimentalists since it has high freedom and low technical barrier compared to box-CARS geometry. At last, some points are notable in Mach-Zehnder interferometers geometry. This geometry uses the same method with the box-CARS geometry to adjust the time delay. Thus, the active phase stability and phase modulation or phase-cycling, which have been used in box-CARS geometry, still are necessary for Mach-Zehnder interferometers geometry.

C. Pump-probe geometry with pulse shaper

With the development of pulse modulation, the pump-probe geometry with pulse shaper (hereinafter referred to as pulse shaper geometry) has been developed [70−75]. The optical design of a pulse shaper is shown in FIG. 4. The pulse shaper geometry can be accomplished by simply replacing the Mach-Zehnder interferometer with a pulse shaper. So, there is almost

DOI:10.1063/1674-0068/cjcp2007125

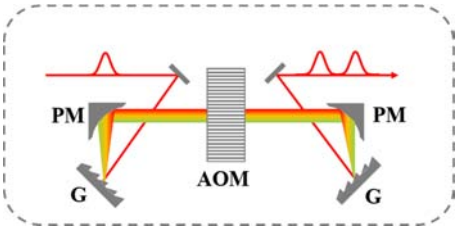

FIG. 4 The optical design of the pulse shaper. PM: parabolic mirror, G: grating, AOM: acoustic optical modulation.

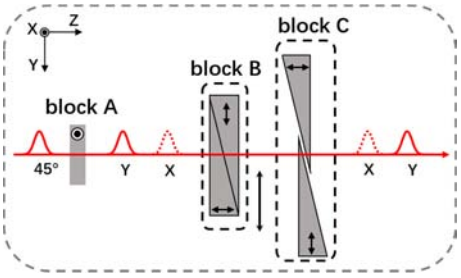

FIG. 5 The optical structure of TWINS. Block A creates the double pulses that have a negative coherence time between them. Block B scans the coherence time into a positive delay. Block C corrects the angular dispersion, front tilt, and tune dispersion. Arrows indicate the orientation of the optical axis in each element. Below each pulse is indicated its polarization. Adapted with permission from Ref.[78] ©The Optical Society.

no technical barrier in the optical design. The pulse shaper is used to create the pump pulse pair and the coherence time τ between them. Because the pump pulse pair always goes through the same optical component, which makes this geometry a representative of the passive phase stabilization approach.

In the pulse shaper geometry, the collinear propagation design of double excitation pulses reduces the technical barrier of 2D FT spectroscopy significantly. In this geometry, the pure absorption signal can be directly acquired, and the rephasing and the non-rephasing signal can also be separated using the phase-cycling method [71]. Besides, compared to the Mach-Zehnder interferometer geometry, the pulse shaper geometry has other unique advantages. First, there is no timing errors and uncertainty in the time zero of the coherence time τ. Second, the phase-cycling method can be implemented to eliminate scattering and separate rephasing and non-rephasing contributions and TG signals. The laser power fluctuations induced noise can be removed using the shot-to-shot phase-cycling method. Third, the rotating frame can be implemented to reduce the acquire time significantly. The details about the rotating frame and phase-cycling method could be found in the literature [62, 76].

Even the pulse shaper geometry has many unique advantages, there are still some drawbacks and limitations. First, The SNR of pulse shaper geometry is lower than the box-CARS geometry because of the influence of the background. Second, the wavelength and bandwidth of the excitation pulse are limited by the pulse shaper. Third, because the pump pulse pair is fully colinear, the separate polarization control for each pump pulse is impossible in this geometry. Thus, it is impossible to experiment with full polarization control. Fourth, the pulse shaper is expensive and fragile. So, it should be more carefully maintained to avoid possible loss and function degradation. Fifth, the 2D FT signal of pulse shaper geometry usually also includes the transient absorption signals produced by pump 1 and pump 2 separately interacting with the probe, which will degrade the data quality. However, different from the Mach-Zehnder interferometer geometry, the phase control ability of pulse shaper could solve the problem easily. As we have mentioned before, the 2D FT spectroscopy signal depends on the phase difference of the excitation pulses, but the background and TA signal are independent of the phase difference. Thus, we could eliminate the background and TA signal without losing the correct 2D FT signal by controlling the phase difference between the excitation pulses using the phase-cycling method [62]. For this purpose, we usually use the following phase-cycling scheme to remove the transient absorption and background scattering: $S(\phi{=}0, \phi{=}0){-}S(\phi{=}0, \phi{=}\pi){+}S(\phi{=}\pi, \phi{=}\pi){-}S(\phi{=}\pi, \phi{=}0)$.

All in all, the development of pulse shaper geometry has a significant meaning to the popularization of the 2D FT spectroscopy in the world. It is a simple and easy choice to operate for the researchers who are familiar with the pump-probe experiment.

D. Pump-probe geometry with TWINS

The pulse shaper geometry is an excellent design to reduce the technical barrier of the 2D FT spectroscopy. However, the high price of pulse shaper could become a heavy burden for many research groups. The pump-probe geometry with TWINS (from now on referred to as TWINS geometry) could be a cost-effective choice by simply replacing the pulse shaper with TWINS [77−80]. FIG. 5 shows the layout of TWINS: it consists mainly of three blocks. When the laser pulse is normally incident into the birefringent crystal, it will split into ordinary polarization and extraordinary polarization laser pulses because of the birefringence, and maintain colinear propagation. Because of the different polarization corresponds to different refractive index, a delay will be introduced between the ordinary and extraordinary pulses. Block A creates the double pump pulses and introduces a negative coherence time τ between them. Then block B introduces a positive coherence time τ which can be tuned by adjusting the position of the birefringent crystals inserted into the beam path to change the optical pathlength of the extraordinary beam. The

DOI:10.1063/1674-0068/cjcp2007125

block C that composed of two wedges is used to correct the angular dispersion, front tilt, and tune dispersion accurately.

The TWINS has a similar function to a pulse shaper, which creates the pump pulse pair and introduces different coherence time τ, while the cost of TWINS is less compared to the pulse shaper. Similar to the pulse shaper, the pump pulse pair generated in TWINS always goes through the same optical components in order to eliminate the phase error between the pump pulses, which makes the TWINS geometry another representative of the passive phase stabilization approach. As a partial colinear geometry, the pure absorption spectrum could also be obtained directly. Moreover, compared to the pulse shaper, the TWINS geometry will not be limited by wavelength and bandwidth of excitation pulses. One weakness of these two designs is that the delay range is short compared to the linear translation stage, usually just several tens picosecond. Nevertheless, it is still enough for most 2D FT spectroscopy experiments. Another disadvantage of TWINS is that the phase-cycling method cannot be applied, and the modulation to a single pulse in the pump pulse pair is impossible.

E. Gradient-assist photo echo (GRAPE) geometry

The 2D FT spectroscopy measurement is often more time-consuming than pump-probe measurement since one dimension is added. Especially in the box-CARS geometry, all coherence times need to be scanned step by step, and the rephasing and non-rephasing spectrum need to acquire separately to get the pure absorption spectrum. Generally, one needs at least ten minutes to acquire a full 2D absorption spectrum map for a given waiting time T. Thus, most existing 2D FT spectrometers cannot measure irreversible processes or samples that are susceptible to the pump pulse. If we can collect a full 2D spectrum in a single laser shot, then we can reduce laser power fluctuations induced noise and measure some irreversible process. Inspired by MD NMR and pulse characterization techniques, Engel and coworkers developed a new 2D FT spectrometer with full nonlinear geometry, which is called GRAPE geometry [81−83]. Different from the box-CARS geometry, the GRAPE geometry has a fantastic feature: single-shot acquiring mode. In the GRAPE geometry, by encoding the coherence time τ into the wavefront of the excitation pulses, the 2D signal with all coherence time could be acquired within a single laser shot [82].

The single-shot feature of GRAPE geometry opens the door to measure the irreversible process. In the meantime, it also significantly reduces the experiment time compared to the traditional 2D FT spectrometer. Because the 2D FT spectroscopy measurement is often susceptible to the environment, the reduction of experiment time will be a benefit to enhance the signal quality, too. However, the rephasing and the non-rephasing signal had to be recorded in the different phase-matching direction, which is a significant drawback that makes it technically more challenging than box-CARS geometry. Besides, compared to the box-CARS geometry, GRAPE geometry requires a higher laser spatial mode quality since it encodes the coherence time into the wavefront of the excitation pulse. Because of the feature of spatial encoding, a 2D camera is necessary for GRAPE. However, the 2D camera usually has a low readout speed, which will limit the laser's repetition frequency for a shot-to-shot measurement. Other drawbacks are the delay range and time step. Because of the spatial encoding feature, the coherence times and steps of GRAPE are fixed [82]. Usually, the range of coherence time is just several picoseconds in the GRAPE. So, the time window is limited in this aspect. Nevertheless, the single-shot feature that reduces acquiring times several orders is very useful for some 2D FT spectroscopy experiments. The GRAPE is still an excellent design and worth to be used for confident experimentalists.

IV. FUTURE AND PERSPECTIVE

2D FT spectroscopy is one of the premier technologies which has significant advantages over other ultrafast spectroscopy methods. Nowadays, the 2D FT spectroscopy in optical frequencies has become a mature technology due to the advances in laser sources and pulse-shaping technology. The application of the 2D FT spectroscopy has been extended to a broad range, for example, Wang and coworkers have demonstrated that 2D infrared (2D IR) spectroscopy could be used to study the correlated molecular motions at the frequencies of overtone transitions of neat liquid [84]. A lot of advanced technologies related to 2D FT spectroscopy have been developed recently, for example, the transient 2D IR has been developed to probe the non-equilibrium state by simply introducing an optical pump to 2D IR spectrometer [85]. As a novel technology, there are still many potential directions waiting us to explore. Below we list some possible future developments in the 2D FT spectroscopy field.

A. Single-shot 2D FT spectroscopy with pump-probe geometry

As we mentioned in the last section, almost all 2D FT spectroscopy is time-consuming and cannot measure the irreversible process. The GRAPE geometry is only an existing optical design that can collect the entire 2D spectrum within a single laser shot. However, it is more technically challenging than the box-CARS geometry, and this creates technical obstacles that are difficult to avoid. So, it will be useful if one can reduce the technical barrier and maintain the single-shot feature at the same time. Getting insight from GRAPE geometry and pulse shaping methods, we believe a single-shot 2D

DOI:10.1063/1674-0068/cjcp2007125

FT spectroscopy with pump-probe geometry should be possible. In this geometry, a new pulse shaper design is needed to produce a pump pulse pair and encode the coherence time into the wavefront by tilting the pump wavefront of one pump pulse. Of course, significant efforts are needed to develop this new pulse shaper, which could change wavefront for each pump pulse separately.

B. Multispectral 2D FT spectroscopy

Nowadays, 2D ES and 2D IR spectroscopy reached maturity and have been implemented in many groups. Recently, one of the developing trends in the 2D FT spectrometer is to extend the temporal observation window and the frequency ranges. A wide time window can be easily scanned using two independent amplifiers seeded by a common oscillator. As to the frequency ranges, one of the frontiers of 2D FT spectroscopy is to expand frequency axes to the broadest possible extent. Nowadays, the 2D FT spectroscopy has expanded to almost the entire electromagnetic spectrum since the development of the pulse shaping methods [86]. The 2D Xray spectroscopy based on the ultrashort X-ray free-electron laser sources is also proposed by Mukamel and coworkers, which can be used to study the non-Born-Oppenheimer dynamics according to their calculations [87−89].

Recently, the interests in the 2D FT spectroscopy of mixing frequency is increasing drastically. The multispectral 2D FT spectroscopy could reveal some hidden structure in distinct spectral bands by combining different spectral regions. For this purpose, the 2D electronic vibrational spectroscopy (2D EV) and 2D vibrational electronic spectroscopy (2D VE) have been demonstrated. The 2D EV technique can be used to explore the electronic-vibrational dynamics, the complex non-radiative pathways, and electron-phonon coupling in the system. And the 2D VE spectroscopy can directly measure how vibrational motions affect electron transfer [90−92]. Recently, many other mixed-frequency 2D FT spectroscopies have also been demonstrated [93, 94]. FIG. 6 depicts an overview of the 2D FT spectroscopy, which is developed or under development. For example, the combination between the THz and the IR or electronic spectroscopy has not been reported yet. The multispectral 2D FT spectroscopy makes the best use of the powerful correlation of 2D FT spectroscopy and is worth paying more attention to. It has become a development trend of the 2D FT spectroscopy now. However, more theoretical explanations are required for these multispectral 2D FT spectroscopy measurements.

C. Chiral 2D FT spectroscopy

Chirality is a ubiquitous characteristic feature of our biological world. The function of large biomolecules depends on their chirality. Optical techniques are most commonly used to detect chirality by measuring the response difference of a sample to left-handed and right-handed circularly polarized light. The time-resolved chiral pump-probe experiment has been accomplished [95−98]. However, the chiral 2D FT spectroscopy is very challenging since the chiral signal is very weak. In 2014, Engel and coworkers acquired the chiral 2D ES in photosynthetic complexes using GRAPE geometry [99]. Researchers theoretically studied how to optimize and isolate the chiral signals in the 2D FT spectroscopy [100, 101]. However, all these researches are based on the full nonlinear geometry, which is very challenging for many groups. Thus, a chiral 2D FT spectroscopy using fully or partially colinear geometries with a low technical barrier will be meaningful. The development of chiral 2D FT spectroscopy will facilitate the chiral structure and dynamics study of large biomolecules. In the meantime, the explanation of the chiral signal is also an important topic that needs more attention.

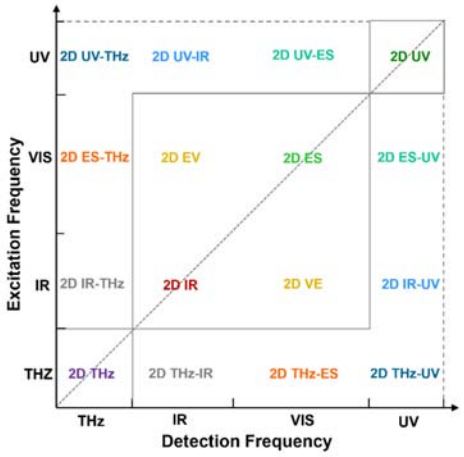

FIG. 6 Overview of the 2D FT spectroscopy developed or under development.

D. Spatially-resolved 2D FT spectroscopy

The inhomogeneous material, photovoltaic materials, 2D material, and single molecular are interesting subjects now. The traditional 2D FT spectroscopy is generally an ensemble measurement which may omit some specificity information of samples. Recently, a fascinating development of single molecular 2D FT measurement technology is implemented, which overcomes the limitations of ensemble measurements in the classical spectroscopy field. Nowadays, the spatially-resolved 2D FT spectroscopy and microscopy have been drawing more and more attention. Tokmakoff and coworkers demonstrated a fully collinear 2D IR microscopy with micrometer spatial resolution [102]. Zanni and coworkers developed a 2D IR microscopy, which could acquire 2D FT imaging of samples and get a full 2D FT spectroscopy from every pixel [103−105]. Because of the excellent SNR and rich spectrum information, the 2D FT

DOI:10.1063/1674-0068/cjcp2007125

microscopy has become a developing trend. In 2018, Oliver and coworkers studied photosynthetic bacteria with spatially-resolved 2D ES, which is a significant progress since it is an *in vivo* measurement [106]. We believe the spatially-resolved 2D FT spectroscopy will become an essential technology in the near future.

V. ACKNOWLEDGMENTS

This work was supported by the National Natural Science Foundation of China (No.91753118 and No.21773012) and the Fundamental Research Funds for Central Universities.

[1] G. R. Fleming, *Chemical Applications of Ultrafast Spectroscopy*, Oxford University Press (1986).
[2] J. Shah, *Ultrafast Spectroscopy of Semiconductors and Semiconductor Nanostructures*, Springer (1996).
[3] R. P. Prasankumar and A. J. Taylor, *Optical Techniques for Solid-State Materials Characterization*, CRC Press (2016).
[4] M. Maiuri, M. Garavelli, and G. Cerullo, J. Am. Chem. Soc. **142**, 3 (2020).
[5] C. J. Fecko, J. D. Eaves, J. J. Loparo, A. Tokmakoff, and P. L. Geissler, Science **301**, 1698 (2003).
[6] T. Brixner, J. Stenger, H. M. Vaswani, M. Cho, R. E. Blankenship, and G. R. Fleming, Nature **434**, 625 (2005).
[7] M. L. Cowan, B. D. Bruner, N. Huse, J. R. Dwyer, B. Chugh, E. T. Nibbering, T. Elsaesser, and R. J. Miller, Nature **434**, 199 (2005).
[8] J. Zheng, K. Kwak, J. Asbury, X. Chen, I. R. Piletic, and M. D. Fayer, Science **309**, 1338 (2005).
[9] J. Zheng, K. Kwak, J. Xie, and M. D. Fayer, Science **313**, 1951 (2006).
[10] C. Kolano, J. Helbing, M. Kozinski, W. Sander, and P. Hamm, Nature **444**, 469 (2006).
[11] J. F. Cahoon, K. R. Sawyer, J. P. Schlegel, and C. B. Harris, Science **319**, 1820 (2008).
[12] K. W. Stone, K. Gundogdu, D. B. Turner, X. Li, S. T. Cundiff, and K. A. Nelson, Science **324**, 1169 (2009).
[13] D. B. Turner and K. A. Nelson, Nature **466**, 1089 (2010).
[14] E. Collini, C. Y. Wong, K. E. Wilk, P. M. Curmi, P. Brumer, and G. D. Scholes, Nature **463**, 644 (2010).
[15] A. Remorino, I. V. Korendovych, Y. Wu, W. F. DeGrado, and R. M. Hochstrasser, Science **332**, 1206 (2011).
[16] C. T. Middleton, P. Marek, P. Cao, C. C. Chiu, S. Singh, A. M. Woys, J. J. de Pablo, D. P. Raleigh, and M. T. Zanni, Nat. Chem. **4**, 355 (2012).
[17] D. G. Kuroda, J. D. Bauman, J. R. Challa, D. Patel, T. Troxler, K. Das, E. Arnold, and R. M. Hochstrasser, Nat. Chem. **5**, 174 (2013).
[18] E. E. Ostroumov, R. M. Mulvaney, R. J. Cogdell, and G. D. Scholes, Science **340**, 52 (2013).
[19] F. D. Fuller, J. Pan, A. Gelzinis, V. Butkus, S. S. Senlik, D. E. Wilcox, C. F. Yocum, L. Valkunas, D. Abramavicius, and J. P. Ogilvie, Nat. Chem. **6**, 706 (2014).
[20] A. Halpin, P. J. Johnson, R. Tempelaar, R. S. Murphy, J. Knoester, T. L. Jansen, and R. J. Miller, Nat. Chem. **6**, 196 (2014).
[21] M. Thamer, L. De Marco, K. Ramasesha, A. Mandal, and A. Tokmakoff, Science **350**, 78 (2015).
[22] G. Moody, C. Kavir Dass, K. Hao, C. H. Chen, L. J. Li, A. Singh, K. Tran, G. Clark, X. Xu, G. Berghäuser, E. Malic, A. Knorr, and X. Li, Nat. Commun. **6**, 8315 (2015).
[23] H. T. Kratochvil, J. K. Carr, K. Matulef, A. W. Annen, H. Li, M. Maj, J. Ostmeyer, A. L. Serrano, H. Raghuraman, S. D. Moran, J. L. Skinner, E. Perozo, B. Roux, F. I. Valiyaveetil, and M. T. Zanni, Science **353**, 1040 (2016).
[24] A. A. Bakulin, S. E. Morgan, T. B. Kehoe, M. W. B. Wilson, A. W. Chin, D. Zigmantas, D. Egorova, and A. Rao, Nat. Chem. **8**, 16 (2016).
[25] F. Dahms, B. P. Fingerhut, E. T. J. Nibbering, E. Pines, and T. Elsaesser, Science **357**, 491 (2017).
[26] H. J. B. Marroux, A. P. Fidler, D. M. Neumark, and S. R. Leone, Sci. Adv. **4**, eaau3783 (2018).
[27] J. J. Hermans, L. Baij, M. Koenis, K. Keune, P. D. Iedema, and S. Woutersen, Sci. Adv. **5**, eaaw3592 (2019).
[28] F. Novelli, J. O. Tollerud, D. Prabhakaran, and J. A. Davis, Sci. Adv. **6**, eaaw9932 (2020).
[29] M. Cho, *Two-Dimensional Optical Spectroscopy*, CRC Press (2009).
[30] P. Hamm and M. Zanni, *Concepts and Methods of 2D Infrared Spectroscopy*, Cambridge University Press (2011).
[31] M. D. Fayer, *Ultrafast Infrared Vibrational Spectroscopy*, CRC Press (2013).
[32] T. Buckup and J. Léonard, *Multidimensional Time-Resolved Spectroscopy*, Springer International Publishing (2019).
[33] J. P. Ogilvie and K. J. Kubarych, *Advances in Atomic Molecular and Optical Physics*, Academic Press, 249 (2009).
[34] D. M. Jonas, Annu. Rev. Phys. Chem. **54**, 425 (2003).
[35] J. P. Wang, Chin. Sci. Bull. **52**, 1221 (2007).
[36] M. Cho, Chem. Rev. **108**, 1331 (2008).
[37] D. Abramavicius, B. Palmieri, D. V. Voronine, F. Sanda, and S. Mukamel, Chem. Rev. **109**, 2350 (2009).
[38] N.S. Ginsberg, Y. C. Cheng, and G. R. Fleming, Acc. Chem. Res. **42**, 1352 (2009).
[39] Z. Jun-Rong, Physics **39**, 162 (2010).
[40] E. Collini, Chem. Soc. Rev. **42**, 4932 (2013).
[41] F. D. Fuller and J. P. Ogilvie, Annu. Rev. Phys. Chem. **66**, 667 (2015).
[42] J. O. Tollerud and J. A. Davis, Prog. Quant. Electron. **55**, 1 (2017).
[43] J. Wang, Int. Rev. Phys. Chem. **36**, 377 (2017).
[44] J. P. Kraack and P. Hamm, Chem. Rev. **117**, 10623 (2017).
[45] H. L. Chen, H. T. Bian, and J. R. Zheng, Acta Phys. Chim. Sin. **33**, 40 (2017).
[46] T. A. A. Oliver, Roy. Soc. Open Sci. **5**, 171425 (2018).
[47] Y. X. Weng, Z. Wang, H. L. Chen, X. Leng, and R. D. Zhu, Acta Phys. Sin. **67**, 12 (2018).
[48] I. Noda, A.E. Dowrey, C. Marcott, G. M. Story, and Y. Ozaki, Appl. Spectrosc. **54**, 236A (2000).
[49] P. Hamm, M. Lim, and R. M. Hochstrasser, J. Phys.

Chem. B **102**, 6123 (1998).
[50] H. Bian, J. Li, X. Wen, Z. Sun, J. Song, W. Zhuang, and J. Zheng, J. Phys. Chem. A **115**, 3357 (2011).
[51] K. Kwak, S. Park, I. J. Finkelstein, and M. D. Fayer, J. Chem. Phys. **127**, 124503 (2007).
[52] S. Park, K. Kwak, and M. D. Fayer, Laser Phys. Lett. **4**, 704 (2007).
[53] K. Kwak, D. E. Rosenfeld, and M. D. Fayer, J. Chem. Phys. **128**, 204505 (2008).
[54] Q. Guo, P. Pagano, Y. L. Li, A. Kohen, and C. M. Cheatum, J. Chem. Phys. **142**, 212427 (2015).
[55] V. Volkov, R. Schanz, and P. Hamm, Opt. Lett. **30**, 2010 (2005).
[56] T. Zhang, C. Borca, X. Li, and S. Cundiff, Opt. Express **13**, 7432 (2005).
[57] F. Milota, V.I. Prokhorenko, T. Mancal, H. von Berlepsch, O. Bixner, H. F. Kauffmann, and J. Hauer, J. Phys. Chem. A **117**, 6007 (2013).
[58] W. Zhu, R. Wang, C. Zhang, G. Wang, Y. Liu, W. Zhao, X. Dai, X. Wang, G. Cerullo, S. Cundiff, and M. Xiao, Opt. Express **25**, 21115 (2017).
[59] F. Ding, P. Mukherjee, and M. T. Zanni, Opt. Lett. **31**, 2918 (2006).
[60] F. D. Fuller, D. E. Wilcox, and J. P. Ogilvie, Opt. Express **22**, 1018 (2014).
[61] J. O. Tollerud, C. R. Hall, and J. A. Davis, Opt. Express **22**, 6719 (2014).
[62] S. H. Shim and M. T. Zanni, Phys. Chem. Chem. Phys. **11**, 748 (2009).
[63] R. Bloem, S. Garrett-Roe, H. Strzalka, P. Hamm, and P. Donaldson, Opt. Express **18**, 27067 (2010).
[64] J. Helbing and P. Hamm, J. Opt. Soc. Am. B **28**, 171 (2010).
[65] I. C. Spector, C. M. Olson, C. J. Huber, and A. M. Massari, Opt. Lett. **40**, 1850 (2015).
[66] R. Augulis and D. Zigmantas, Opt. Express **19**, 13126 (2011).
[67] M. Khalil, N. Demirdoven, and A. Tokmakoff, Phys. Rev. Lett. **90**, 047401 (2003).
[68] R. Zhu, S. Yue, H. Li, X. Leng, Z. Wang, H. Chen, and Y. Weng, Optics Express **27**, 15474 (2019).
[69] L. P. Deflores, R. A. Nicodemus, and A. Tokmakoff, Opt. Lett. **32**, 2966 (2007).
[70] E. M. Grumstrup, S. H. Shim, M. A. Montgomery, N. H. Damrauer, and M. T. Zanni, Opt. Express **15**, 16681 (2007).
[71] J. A. Myers, K. L. Lewis, P. F. Tekavec, and J. P. Ogilvie, Opt. Express **16**, 17420 (2008).
[72] P. F. Tekavec, J. A. Myers, K. L. Lewis, and J. P. Ogilvie, Opt. Lett. **34**, 1390 (2009).
[73] C. T. Middleton, A. M. Woys, S. S. Mukherjee, and M. T. Zanni, Methods **52**, 12 (2010).
[74] N. M. Kearns, R. D. Mehlenbacher, A. C. Jones, and M. T. Zanni, Opt. Express **25**, 7869 (2017).
[75] A. Ghosh, A. L. Serrano, T. A. Oudenhoven, J. S. Ostrander, E. C. Eklund, A. F. Blair, and M. T. Zanni, Opt. Lett. **41**, 524 (2016).
[76] Z. Zhang, K. L. Wells, E. W. J. Hyland, and H. S. Tan, Chem. Phys. Lett. **550**, 156 (2012).
[77] D. Brida, C. Manzoni, and G. Cerullo, Opt. Lett. **37**, 3027 (2012).
[78] J. Rehault, M. Maiuri, C. Manzoni, D. Brida, J. Helbing, and G. Cerullo, Opt. Express **22**, 9063 (2014).
[79] J. Rehault, M. Maiuri, A. Oriana, and G. Cerullo, Rev. Sci. Instrum. **85**, 123107 (2014).
[80] R. Borrego-Varillas, A. Oriana, L. Ganzer, A. Trifonov, I. Buchvarov, C. Manzoni, and G. Cerullo, Opt. Express **24**, 28491 (2016).
[81] E. Harel, A. F. Fidler, and G. S. Engel, Proc. Natl. Acad. Sci. USA **107**, 16444 (2010).
[82] E. Harel, A. F. Fidler, and G. S. Engel, J. Phys. Chem. A **115**, 3787 (2011).
[83] V. P. Singh, A. F. Fidler, B. S. Rolczynski, and G. S. Engel, J. Chem. Phys. **139**, 084201 (2013).
[84] D. Li, F. Yang, C. Han, J. Zhao, and J. Wang, J. Phys. Chem. Lett. **3**, 3665 (2012).
[85] J. Bredenbeck, J. Helbing, R. Behrendt, C. Renner, L. Moroder, J. Wachtveitl, and P. Hamm, J. Phys. Chem. B **107**, 8654 (2003).
[86] Y. Song, A. Konar, R. Sechrist, V. P. Roy, R. Duan, J. Dziurgot, V. Policht, Y. A. Matutes, K. J. Kubarych, and J. P. Ogilvie, Rev. Sci. Instrum. **90**, 013108 (2019).
[87] S. Mukamel, D. Healion, Y. Zhang, and J. D. Biggs, Annu. Rev. Phys. Chem. **64**, 101 (2013).
[88] M. Kowalewski, K. Bennett, K. E. Dorfman, and S. Mukamel, Phys. Rev. Lett. **115**, 193003 (2015).
[89] K. Bennett, Y. Zhang, M. Kowalewski, W. Hua, and S. Mukamel, Phys. Scripta T **169**, 014002 (2016).
[90] T. A. A. Oliver, N. H. C. Lewis, and G. R. Fleming, Proc. Natl. Acad. Sci. **111**, 16628 (2014).
[91] T. L. Courtney, Z. W. Fox, L. Estergreen, and M. Khalil, J. Phys. Chem. Lett. **6**, 1286 (2015).
[92] T. L. Courtney, Z. W. Fox, K. M. Slenkamp, and M. Khalil, J. Chem. Phys. **143**, 154201 (2015).
[93] P. Hamm and J. Savolainen, J. Chem. Phys. **136**, 094516 (2012).
[94] I. A. Finneran, R. Welsch, M. A. Allodi, T. F. Miller 3rd, and G. A. Blake, Proc. Natl. Acad. Sci. USA **113**, 6857 (2016).
[95] C. Niezborala and F. Hache, J. Opt. Soc. Am. B **23**, 2418 (2006).
[96] L. Mangot, G. Taupier, M. Romeo, A. Boeglin, O. Cregut, and K. D. H. Dorkenoo, Opt. Lett. **35**, 381 (2010).
[97] A. Trifonov, I. Buchvarov, A. Lohr, F. Wurthner, and T. Fiebig, Rev. Sci. Instrum. **81**, 043104 (2010).
[98] K. Hiramatsu and T. Nagata, J. Chem. Phys. **143**, 121102 (2015).
[99] A. F. Fidler, V. P. Singh, P. D. Long, P. D. Dahlberg, and G. S. Engel, Nat. Commun. **5**, 3286 (2014).
[100] B. Dutta and J. Helbing, Opt. Express **23**, 16449 (2015).
[101] D. I. Holdaway, E. Collini, and A. Olaya-Castro, Opt. Express **25**, 6383 (2017).
[102] C. R. Baiz, D. Schach, and A. Tokmakoff, Opt. Express **22**, 18724 (2014).
[103] A. L. Serrano, A. Ghosh, J. S. Ostrander, and M. T. Zanni, Opt. Express **23**, 17815 (2015).
[104] J. S. Ostrander, A. L. Serrano, A. Ghosh, and M. T. Zanni, ACS Photon. **3**, 1315 (2016).
[105] A. C. Jones, N. M. Kearns, M. B. Kunz, J. T. Flach, and M. T. Zanni, J. Phys. Chem. A **123**, 10824 (2019).
[106] V. Tiwari, Y. A. Matutes, A. T. Gardiner, T. L. C. Jansen, R. J. Cogdell, and J. P. Ogilvie, Nat. Commun. **9**, 4219 (2018).

DOI:10.1063/1674-0068/cjcp2007125